arXiv:1007.4717v1 [cond-mat.quant-gas] 27 Jul 2010

Dynamics of a cold trapped ion in a Bose-Einstein condensate

Stefan Schmid,[1,2] Arne Härter,[1,2] and Johannes Hecker Denschlag[1,2]
[1]*Institut für Quantenmaterie, Universität Ulm, 89069 Ulm, Germany*
[2]*Institut für Experimentalphysik und Zentrum für Quantenphysik, Universität Innsbruck, 6020 Innsbruck, Austria*

(Dated: July 28, 2010)

We investigate the interaction of a laser-cooled trapped ion (Ba$^+$ or Rb$^+$) with an optically confined ^{87}Rb Bose-Einstein condensate (BEC). The system features interesting dynamics of the ion and the atom cloud as determined by their collisions and their motion in their respective traps. Elastic as well as inelastic processes are observed and their respective cross sections are determined. We demonstrate that a single ion can be used to probe the density profile of an ultracold atom cloud.

PACS numbers: 34.50.-s, 37.10.-x, 03.75.Hh, 34.70.+e

The realization of a charged quantum gas, formed by laser-cooled, trapped ions and ultracold neutral atoms, offers intriguing perspectives for a variety of novel experiments. In addition to studying atom-ion collisions and chemical reactions in a regime where only one or few partial waves contribute, interesting phenomena such as charge transport in the ultracold domain [1], polaron-type physics [2–4], and novel atom-ion bound states [5] can be investigated. Further, the production of cold, charged molecules in a well-defined quantum state is an important goal in molecular physics [6, 7]. Techniques and tools that are widely used to control neutral atomic quantum gases, e.g. Feshbach resonances [8], may be employed in atom-ion collisions as well [9]. First observations of cold collisions with trapped atoms and ions in the mK regime have been made using Yb$^+$ ions and a magneto-optical trap for Yb [10, 11] and very recently with a Bose-Einstein condensate (Yb$^+$, Rb) [12]. Here we present our investigations where we use a defined small number of Ba$^+$ or Rb$^+$ ions which are immersed in an ultracold cloud of Rb atoms, which is either Bose-Einstein condensed or at sub-µK temperature. We find that at our current settings micromotion of the trapped ions plays an important role in our experiments. The elastic cross sections are large as expected. Inelastic processes are in general strongly suppressed, which is important for planned future experiments. Charge transfer is directly identified in our experiments and found to be the dominant inelastic collision channel. As a first application we show how a trapped ion can be used to locally probe the density profile of a condensate.

In the inhomogeneous electrical field of an ion, a neutral atom is polarized and attracted towards the ion. This interaction can be expressed as a long-range polarization potential $V(r) = -C_4/2r^4$ with $C_4 = q^2\alpha/4\pi\varepsilon_0$, where q is the charge of the ion and α the dc polarizability of the atom. The characteristic radius of the potential is given by $r^* = \sqrt{\mu C_4/\hbar}$, where μ is the reduced mass. For a ^{87}Rb atom ($\alpha = 4.7 \times 10^{-31}\,\mathrm{m}^3$ [14]) interacting with a ^{138}Ba$^+$ ion, this characteristic radius is $r^* = 295\,\mathrm{nm}$. This is much larger than the typical length scale of the neutral atom-atom interaction potential as given by the van der Waals radius, which for ^{87}Rb is $R_{vdW} \approx 4\,\mathrm{nm}$ [8]. For collision energies E above $k_\mathrm{B} \times 100\,\mu\mathrm{K}$, the cross section for elastic scattering can be approximated by the semi-classical estimate $\sigma_\mathrm{el} = \pi(\mu C_4/\hbar^2)^{1/3}(1+\pi^2/16)E^{-1/3}$ [15]. At lower energies a full quantum mechanical treatment is necessary, which takes into account individual partial waves. In addition to elastic collisions, inelastic processes can also occur, such as charge transfer $\mathrm{Rb} + \mathrm{Ba}^+ \to \mathrm{Rb}^+ + \mathrm{Ba}$ or molecule formation $\mathrm{Rb} + \mathrm{Rb} + \mathrm{Ba}^+ \to \mathrm{Rb} + (\mathrm{BaRb})^+$.

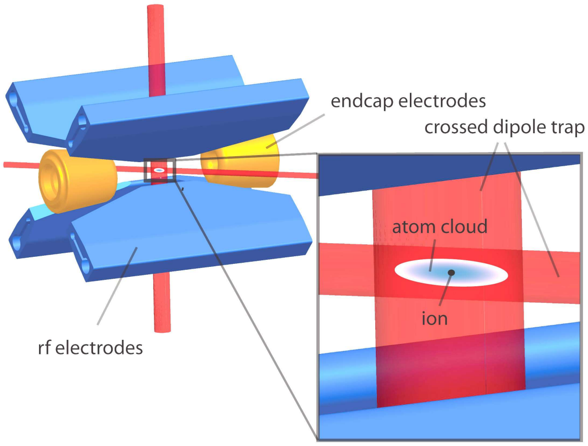

FIG. 1. Combined atom-ion trap: A linear radiofrequency Paul trap is used to store ions [20], whereas the ultracold atoms are confined in a crossed optical dipole trap. By precisely overlapping the positions of these two traps, a single ion can be immersed into the center of the ultracold neutral atom cloud.

Here we present the first results obtained with our novel hybrid apparatus, where both species (Ba$^+$, Rb) are first trapped and cooled in separate parts of a UHV chamber in order to minimize mutual disturbance and are then brought together. We use a linear Paul trap into which we can load a well-defined number of ^{138}Ba$^+$ ions (typically 1) by photoionizing neutral Ba atoms from a getter source. Photoionization is done with a diode laser at 413 nm, which drives a resonant two-photon transition from the ground state to the continuum via the $^3\mathrm{D}_1$ state. The ^{138}Ba$^+$ ion which has no hyperfine structure is Doppler-cooled to mK temperatures using a laser at 493 nm. Another laser at 650 nm repumps from a metastable $\mathrm{D}_{3/2}$ state. The ion's fluorescence is collected with a lens of NA = 0.2 and then detected using an electron multiplying charged-coupled device (EMCDD) camera. The linear Paul trap (see Fig. 1) consists of four blade electrodes, which are placed at a distance of 2 mm from the trap axis, and two endcap electrodes at a distance of 7 mm from the trap center. It is operated with a radiofrequency (rf) drive of $\Omega = 2\pi\times5.24\,\mathrm{MHz}$ with an amplitude of $1400\,\mathrm{V_{pp}}$ and a dc endcap voltage of about 100 V. With these parameters we measure the axial and the radial trap frequencies to be $\omega_{\mathrm{I,ax}} \approx 2\pi\times80\,\mathrm{kHz}$ and $\omega_{\mathrm{I,rad}} \approx 2\pi\times200\,\mathrm{kHz}$, respectively.

The sample of ultracold Rb atoms is prepared similarly as described in [16]. Atoms from a magneto-optical trap are magnetically transferred over a distance of 43 cm into a quadrupole Ioffe configuration (QUIC) trap. Evaporative cooling yields a cloud of 3×10^6 ^{87}Rb atoms in state $|F=1,\ m_F=-1\rangle$ at a temperature of about $1\,\mu$K. From the magnetic trap we load the atom cloud into a vertical 1-dimensional optical lattice trap formed by two counterpropagating laser beams (diameter $\approx 500\,\mu$m) at a wavelength of 1064 nm with a total power of 2 W. We use the lattice as an elevator to transport the ultracold atoms upwards into the center of the Paul trap which is located 30 cm above the QUIC trap. The lattice is moved by changing the relative detuning of the two beams in a controlled manner [17]. The transport efficiency reaches more than 60%. During transport the depth of the lattice is sufficiently small ($\approx k_{\mathrm{B}}\times10\,\mu\mathrm{K}$) so that evaporation keeps the atom temperature at about $1\,\mu$K. After transport the atomic sample is loaded into a crossed optical dipole trap ($\lambda = 1064\,\mathrm{nm}$). By lowering the trap depth, we evaporatively cool the atoms and end up with a BEC of about 10^5 atoms confined in a dipole trap with trap frequencies of about $\omega_{\mathrm{Rb}}^{(x,y,z)} = (60\,\mathrm{Hz}, 60\,\mathrm{Hz}, 8\,\mathrm{Hz})$. The condensate is detected via standard absorption imaging.

The BEC is initially located about $300\,\mu$m away from the ion. We move the ion within 2 ms along the Paul trap axis into the BEC by changing the endcap voltages. The cooling lasers for the ion are switched off in order to ensure that the ion relaxes into its electronic ground state $|F=1/2,\ m_F=\pm1/2\rangle$ and to avoid changes in the atom-ion collision dynamics due to the cooling radiation.

Initially the temperature of the ion is on the order of a few mK, which is much larger than the optical trap depth of about $k_B\times1\,\mu$K. Thus almost any collision with a cold atom leads to the atom being lost from the trap.

As a consequence, one could naively expect, that the atom loss stops after a few collisions, once the ion is sympathetically cooled to atomic temperatures. However, when we measure the number of Rb atoms remaining in the trap as a function of the interaction time, we find a continuous loss of atoms (Fig. 2). It is the driven micromotion of the rf trap, which [18] is responsible for this continuing loss. In an atom-ion collision, energy can be redistributed among all motional degrees of freedom, enabling also the flux of micromotion energy to secular motion. After each collision, micromotion is quickly restored by the driving rf field. An equilibrium between the energy that is inserted by the driving field and the energy taken away by the lost atoms is reached. Thus the minimal temperature of a sympathetically-cooled ion stored in a rf trap is determined by the amount of micromotion of the ion [19]. Stray electric fields which shift the ion position away from the zero of the rf potential increase micromotion, leading to the so-called excess micromotion [18]. By applying dc electric fields along the radial direction this part of the micromotion is tunable.

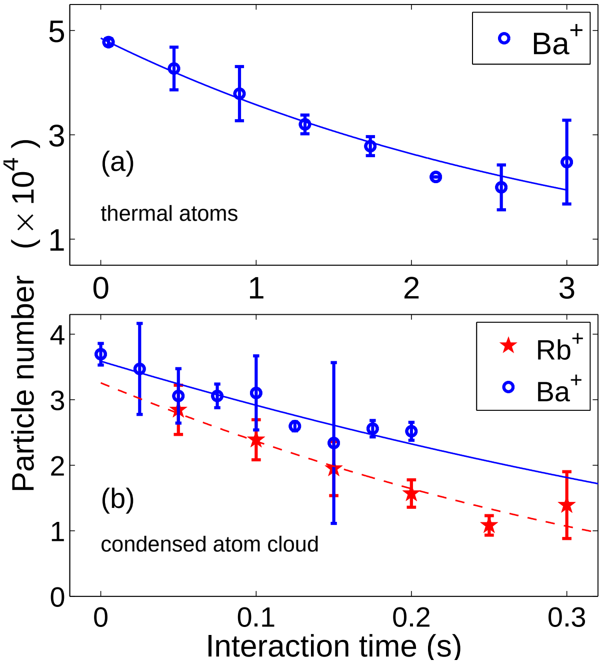

FIG. 2. Number of remaining Rb atoms as a function of time as a sample of Rb atoms interacts with an ion. **(a)** A single Ba$^+$ ion is immersed into the center of a thermal Rb cloud. The line is an exponential decay fit. **(b)** A single ion (Ba$^+$ or Rb$^+$) is immersed in a Rb Bose-Einstein condensate. The lines are fits based on our simple model described in the text.

Fig. 2 shows the elastic collision measurements with either (a) a thermal cloud of atoms (temperature $T_{\mathrm{Rb}}=80\,\mathrm{nK}$, which is just above T_c) or (b) a BEC. In the following we analyze these data in detail starting out with the case for thermal atoms. In general, we have checked that losses due to collisions with the background gas are negligible. The loss of atoms is then described by $\dot{N} = -\tilde{n}\sigma_{\mathrm{el}}v_{\mathrm{I}}$, where $\tilde{n}$ is the density of the atom cloud at the position of the ion, σ_{el} the elastic atom-ion cross section and v_{I} the velocity of the ion. In principal all three quantities are unknown. Based on our measurements and additional constraints of the following model we can still give estimates for them.

It is important to note that the density profile of the atom cloud is depleted locally due to the collisions with the well-localized ion. According to its mass m_{I}, energy $E_{\mathrm{I}} = m_{\mathrm{I}}v_{\mathrm{I}}^2/2$, and trap frequency ω_{I} the ion will be localized inside a region (which for simplicity we choose to be spherical) of radius $r_0 = \sqrt{E_{\mathrm{I}}/m_{\mathrm{I}}\omega_{\mathrm{I}}^2}$. Inside this sphere we assume a homogeneous density $\tilde{n}$. Right outside the sphere, the density is given by

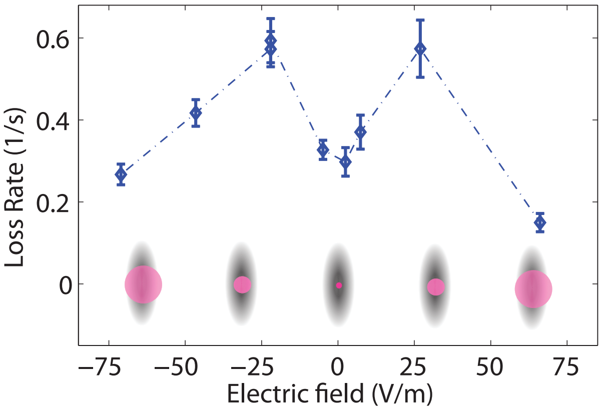

FIG. 3. Loss rate of a thermal atom cloud when a static electric field is applied. In the presence of a field, the energy of the Ba^+ ion and thus the amplitude of its secular motion are increased. As a result the sphere of depletion becomes larger, leading to an enhanced atom loss rate. For fields $|\mathscr{E}_{\rm dc}| > 30\,\mathrm{V/m}$, the amplitude of the secular motion is so large, that the ion spends a significant amount of time in a region of lower atom density. Therefore the loss rate decreases at high fields.

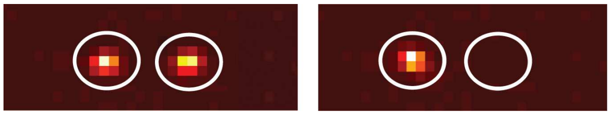

FIG. 4. *Left*: Fluorescence image of two Ba^+ ions. *Right*: Fluorescence of one $^{138}\mathrm{Ba}^+$ next to an unknown dark ion . We infer the existence of the dark ion from the position of the Ba^+.

$n = N\bar{\omega}_{\rm Rb}^3 (m_{\rm Rb}/2\pi k_B T_{\rm Rb})^{3/2}$, which is the peak density of a thermal cloud of Rb atoms (mass $m_{\rm Rb}$) confined in a harmonic trap with mean trap frequency $\bar{\omega}_{\rm Rb} = (\omega_{\rm Rb}^{(x)}\omega_{\rm Rb}^{(y)}\omega_{\rm Rb}^{(z)})^{1/3}$. The measured atom loss $\dot{N}$, which at $t = 0$ is $\dot{N} = 1.5\times 10^4\,\mathrm{s}^{-1}$ (as can be read off from Fig. 2), must match the net flux of atoms into the “sphere of depletion”, leading to the balance condition $\dot{N} = \pi r_0^2 (n - \tilde{n}) v_{\rm th}$. Here the thermal velocity of the atoms is given by $v_{\rm th} = \sqrt{k_B T_{\rm Rb}/8\pi m_{\rm Rb}}$. By setting $\tilde{n} = 0$ in the balance condition we get a lower bound for the ion energy, which for our parameters is equal to $k_B \times 17\,\mathrm{mK}$. We can also estimate an upper limit of the ion energy from our method of compensating micromotion. The compensation is based on minimizing the position shift of the ion when the rf amplitude is changed. With this method we can reduce the DC electric field at the position of the ion to below $4\,\mathrm{V/m}$, corresponding to a maximum ion energy of $k_B \times 40\,\mathrm{mK}$ [18]. By taking the midpoint between the two bounds we estimate the ion energy to be about $k_B \times 30\,\mathrm{mK}$. Plugging this energy into the expressions above we get $r_0 \approx 1.45\,\mu\mathrm{m}$ and a density of $\tilde{n} \approx 0.45\,n$. Moreover we can determine the cross section $\sigma_{\rm el}$ to be $1.9\times 10^{-14}\,\mathrm{m}^2$. This value is in rough agreement with the semiclassical estimate $\sigma_{\rm el}^{\rm semi} = 9\times 10^{-15}\,\mathrm{m}^2$.

A slightly different analysis can be done for the measurement with the BEC shown in Fig. 2(b). Again, collisions of the atoms with the trapped ion will lead to a sphere of depletion within the condensate. However, the flux of atoms into the sphere is now driven by mean field pressure rather than thermal motion. From numerical calculations using a 3D Gross-Pitaevskii equation with an absorptive (imaginary) potential term, we find that the flux into the sphere can be approximated by $4\pi r_0^2 \tilde{n} v_e$, as long as $\tilde{n} \gtrsim 0.1\,n$. Here $v_e = 4\hbar\sqrt{2\pi a(n-\tilde{n})}/m_{\rm Rb}$ is the velocity with which the atoms enter the sphere, $a = 5.61\,\mathrm{nm}$ is the Rb-Rb s-wave scattering length and $n = \left(15 m_{\rm Rb}^3 \bar{\omega}_{\rm Rb}^3 N/\hbar a^{3/2}\right)^{2/5}/8\pi$ is the peak density of the condensate. By equating the net flux to the measured lossrate of the BEC at $t = 0$, $\dot{N} = 8\times 10^4\,\mathrm{s}^{-1}$ (see Fig. 2), we find that the ion energy has to be larger than $k_{\rm B} \times 1\,\mathrm{mK}$. Our analysis shows, that on the other hand the ion energy has to be smaller than in the thermal case. Indeed, to minimize the temperature of the trapped ion, a comparatively large effort was made to compensate micromotion for the experiments with the BEC. Given that $\sigma_{\rm el}/\sigma_{\rm el}^{\rm semi} \approx 2$ as in the thermal case, our data suggests a reasonable ion energy of about $k_{\rm B} \times 5\,\mathrm{mK}$. This implies $r_0 \approx 0.8\,\mu\mathrm{m}$, a density of $\tilde{n} \approx 0.1\,n$ and a cross section of $\sigma_{\rm el} \approx 3.1\times 10^{-14}\,\mathrm{m}^2$. We also measured the loss rate for a single Rb^+ ion and found it to be about the same as with Ba^+ (Fig. 2). This is not surprising, since the atom loss rate depends only weakly on the ionic mass and the inner structure of the ion is irrelevant in the semiclassical regime.

Following this discussion, we expect the net flux into the sphere and thus the atom loss rate to rise when we intentionally increase the dc electric field. For small fields this is also what we observe in the experiment (Fig. 3). The maximum loss rate is observed at an electric field of $\mathscr{E}_{\rm dc} \approx 30\,\mathrm{V/m}$, where the amplitude of the ion’s secular motion is $r_0 \approx 20\,\mu\mathrm{m}$. This value is comparable to the size of the atom cloud, which has an extension of about $15\,\mu\mathrm{m}$ along the radial and $80\,\mu\mathrm{m}$ along the axial direction. The model of a well-localized ion and a sphere of depletion is clearly no longer valid in this regime. We explain the decrease of the atom loss rate for even higher fields by the fact that the ion spends a significant amount of time in regions of lower atom density.

In addition to the elastic processes discussed so far, we have also investigated inelastic atom-ion collisions. For this we load two $^{138}\mathrm{Ba}^+$ ions into the ion trap. Typically after a time corresponding to 10^4-10^5 elastic atom-ion collisions, the fluorescence of one of the Ba^+ ions is lost (Fig. 4). Since the position of the remaining bright Ba^+ ion does not change, we infer that the other Ba^+ ion has been replaced by an unknown dark ion formed in a reaction. We can determine the mass of the dark ion by measuring the radial center-of-mass (COM) trap frequency. For this we modulate the amplitude of the rf voltage. When the modulation frequency is equal to the trap frequency the ion motion is resonantly excited and a drop of the Ba^+ fluorescence signal is observed. We only observe two resonance frequencies at $245\,\mathrm{kHz}$ and $400\,\mathrm{kHz}$. We have checked that Ba^+ gives rise to the $245\,\mathrm{kHz}$ resonance. Using the scaling properties of the analytic expression for the COM mode [20], the $400\,\mathrm{kHz}$ resonance then corresponds to the mass of $^{87}\mathrm{Rb}^+$. We conclude that the dominant

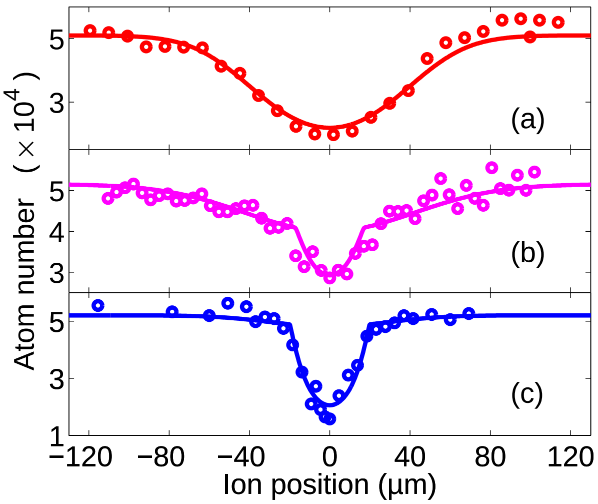

FIG. 5. Number of Rb atoms remaining in the trap depending on the position of the Rb^+ ion relative to the center of the atom cloud. The measurement is performed with (a) a thermal cloud, (b) a partially condensed cloud and (c) an almost pure Bose-Einstein condensate. The interaction time was (a) 1.5 s, (b) 1 s and (c) 0.5 s. The solid lines are fits, where the ion energy E_I and the atom temperature T_{Rb} are used as free fit parameters.

inelastic process in our system is the charge transfer process $\mathrm{Rb}+\mathrm{Ba}^+ \rightarrow \mathrm{Rb}^+ + \mathrm{Ba}$ with a cross section $\sigma_{\mathrm{ch.ex.}}$ ranging between $10^{-19}\,\mathrm{m}^2$ and $10^{-18}\,\mathrm{m}^2$. Our charge transfer results are comparable to the ones observed for the heteronuclear case of (Rb, Yb^+) [13]. Homonuclear charge transfer rates are orders of magnitudes higher [11]. In our case the charge transfer is predicted to be dominantly radiative, where a photon carries away most of the 1 eV of energy released in this reaction [21]. The Rb^+ ion can be stored in the trap for hours, even without any type of cooling, which opens up perspectives to study energetically resonant (Rb, Rb^+) collisions.

We now show how a single ion may be used to locally probe the atomic density distribution. By controlling the endcap voltage a single Rb^+ ion is moved stepwise across the atom cloud and at each position x the atom loss is measured for a given interaction time (Fig. 5). The measurement is performed with various Rb clouds with different condensate fractions. We can theoretically reproduce the data shown in Fig. 5 with our model, which demonstrates our quantitative understanding of the dynamics. For this we write the total atom loss of a partly condensed cloud as a sum of the individual losses from the BEC and the thermal cloud as discussed before. For numerical calculations we choose $\sigma_{\mathrm{el}} = 3\times 10^{-14}\,\mathrm{m}^2$ and make use of the well-known density profiles for a thermal and a condensed atom cloud confined in a harmonic trap. The thermal component and BEC are in equilibrium and obey $N_c/N = 1-(T_{\mathrm{Rb}}/T_c)^3$ where T_c is the critical temperature and N_c/N is the condensate fraction which changes with time. The temperature T_{Rb} of the atomic sample is constant, as determined by the optical trap depth. It is used as a free fit parameter in our model together with the ion energy E_I, which we keep fixed for all three measurements. Fig. 5 depicts the total number of remaining particles $N(x)$ as a function of the ion's position x. The values for T_{Rb} obtained from the fit (a) 50 nK, (b) 35 nK and (c) 25 nK are in nice agreement with the temperatures determined separately in time-of-flight measurements. Moreover the fit suggests $E_I \approx k_B \times 14\,\mathrm{mK}$, which is in the same range as the temperatures found in the Ba^+ experiments. The ion probe features a spatial resolution on the µm scale and has advantages compared to absorption imaging which integrates over the line of sight.

In conclusion we have immersed cold trapped ions in a sea of ultracold neutral atoms in a novel hybrid apparatus with high spatial and temporal control. We have investigated the dynamics of the atom-ion system and have extracted first elastic and inelastic collision properties. In our present setup the collision energies are determined by the ionic excess micromotion, which we plan to minimize for future experiments in the ultracold regime.

The authors would like to thank Albert Frisch and Sascha Hoinka for their help during the early stage of the experiment and Thomas Busch, Tommaso Calarco, Robin Côté, Bretislav Friedrich, Bo Gao, Zbigniew Idziaszek, Tobias Schätz, Wolfgang Schnitzler, and Jaques Tempère for helpful discussions and support. We are grateful to Rudi Grimm for generous support and to Michael Drewsen and the group of Rainer Blatt for advice on the design of the ion trap. This work was supported by the Austrian Science Fund (FWF). S.S. acknowledges support from the Austrian Academy of Sciences within the DOC doctorial research fellowship program.

---

[1] R. Côté, Phys. Rev. Lett. **85**, 5316 (2000).
[2] P. Massignan, C. J. Pethick, and H. Smith, Phys. Rev. A **71**, 023606 (2005).
[3] R. M. Kalas, and D. Blume, Phys. Rev. A **73**, 043608 (2006).
[4] F. M. Cucchietti, and E. Timmermans, Phys. Rev. Lett. **96**, 210401 (2006).
[5] R. Côté, V. Kharchenko, and M. D. Lukin, Phys. Rev. Lett. **89**, 093001 (2002).
[6] P. F. Staanum, K. Hojbjerre, P. Skyt, A. Hansen, and M. Drewsen, Nat. Phys. **6**, 271 (2010).
[7] T. Schneider, B. Roth, H. Duncker, I. Ernsting, and S. Schiller, Nat. Phys. **6**, 275 (2010).
[8] C. Chin, R. Grimm, P. S. Julienne, and E. Tiesinga, Rev. Mod. Phys. **82**, 1225 (2010).
[9] Z. Idziaszek, T. Calarco, P. S. Julienne, and A. Simoni, Phys. Rev. A **79**, 010702 (2009).
[10] M. Cetina, A. Grier, J. Campbell, I. Chuang, and V. Vuletic, Phys. Rev. A **76**, 041401 (2007).
[11] A. T. Grier, M. Cetina, F. Orucevic, and V. Vuletic, Phys. Rev. Lett. **102**, 223201 (2009).
[12] C. Zipkes, S. Palzer, C. Sias, and M. Köhl, Nature **464**, 388-391 (2010).
[13] C. Zipkes, S. Palzer, L. Ratschbacher, C. Sias, and M. Köhl, arXiv:1005.3846v1 (2010).
[14] R. Teachout, and R. Pack, Atomic Data **3**, 195 (1971).

[15] R. Côté, and A Dalgarno, Phys. Rev. A **62**, 012709 (2000).

[16] G. Thalhammer, M. Theis, K. Winkler, R. Grimm, and H. Hecker Denschlag, Phys. Rev. A **71**, 033403 (2005).

[17] S. Schmid, G. Thalhammer, K. Winkler, F. Lang, and J. Hecker Denschlag, New. J. Phys. **8**, 159 (2006).

[18] D. J. Berkeland, J. D. Miller, J. C. Bergquist, W. M. Itano, and D. J. Wineland, J. App. Phys. **83**, 5025-5033 (1998).

[19] F. G. Major, and H. G. Dehmelt, Phys. Rev. **170**, 91 (1968).

[20] D. Wineland, C. Monroe, W.M. Itano, D. Leibfried, B.E. King, and D.M. Meekhof, J. Res. Natl. Inst. Stand. Technol. **103**, 259 (1998).

[21] O.P. Makarov, R. Côté, H. Michels, and W.W. Smith, Phys. Rev. A **67**, 042705 (2003).